Published in "Chemical Geology 269(3-4): 210-219, 2010"
which should be cited to refer to this work.

Stable isotope profiles (Ca, O, C) through modern brachiopod shells of *T. septentrionalis* and *G. vitreus*: Implications for calcium isotope paleo-ocean chemistry

Katja von Allmen [a], Thomas F. Nägler [b], Thomas Pettke [b], Dorothee Hippler [c], Erika Griesshaber [d], Alan Logan [e], Anton Eisenhauer [f], Elias Samankassou [a,*]

[a] *Department of Geosciences, Chemin du Musée 6, University of Fribourg, CH-1700 Fribourg, Switzerland*
[b] *Institute of Geological Science, Baltzerstr. 1+3, University of Bern, CH-3012 Bern, Switzerland*
[c] *Dept. of Sedimentology and Marine Geology, VU University of Amsterdam, de Boelelaan 1085, 1018 HV Amsterdam, The Netherlands*
[d] *Dept. of Earth- and Environmental Sciences, Ludwig-Maximilian University, Theresienstr. 41, 80333 Munich, Germany*
[e] *Centre for Coastal Studies, University of New Brunswick, 100 Tucker Park Road, Saint John NB, Canada E2L 4L5*
[f] *Leibniz Institute of Marine Sciences, IFM-GEOMAR, Wischhofstr. 1-3, D-24148 Kiel, Germany*

Brachiopod shells are widely used as an archive to reconstruct elemental and isotopic composition of seawater. Studies, focused on oxygen and carbon isotopes over the last decades, are increasingly extending to the emerging calcium isotope system. To date, only little attention has been paid to test the reliability of fossil brachiopods on their modern counterparts.

In this context, the present study investigates two modern brachiopods, *Terebratulina septentrionalis* (eastern Canada, 5–30 m depth, 7.1 °C seasonal temperature variation, two-layer shell) and *Gryphus vitreus* (northern Mediterranean, 200 m depth, constant all-year round temperature, three-layer shell). Both species were sampled along the ontogenetic growth direction and calcium, oxygen, and carbon isotopes as well as elemental concentration were measured. Calcium isotopes were analyzed on TIMS. The elemental composition was analyzed by LA-ICP-MS and ICP-AES.

The results indicate an intra-specimen $\delta^{44/40}$Ca variation ranging from 0.16 to 0.33‰, pointing to a fairly homogenous distribution of calcium isotopes in brachiopod shells. However, in the light of the suggested 0.7‰ increase in calcium isotopes over the Phanerozoic such intra-specimen variations constrain ocean reconstruction. $\delta^{44/40}$Ca values of *T. septentrionalis* do not seem to be affected by growth rate. Calcium isotopic values of *G. vitreus* are heavy in the central part of the shell and trend towards lighter values in peripheral areas approaching the maximum isotopic composition of *T. septentrionalis*. The maximum inter-species $\delta^{44/40}$Ca difference of 0.62‰ between *T. septentrionalis* and *G. vitreus* indicates that care should be taken when using different taxa, species with different strontium content or brachiopods with specialized shell structure, such as *G. vitreus*, for ocean water reconstruction in terms of Ca isotopic composition. *T. septentrionalis* may record Ca isotopic fractionation related to seasonal seawater temperature variations in its shell but this is difficult to resolve at the current analytical precision. Average δ^{18}O-derived temperatures of the two investigated species are close to on-site measured temperatures.

1. Introduction

Recently, the number of studies on the calcium isotope system of skeletal carbonates has rapidly increased. The studies investigate paleoceanographic and paleoclimatic changes, stratigraphic correlations and biological fractionation (e.g., Immenhauser et al., 2005; Gussone et al., 2006; Farkaš et al., 2007a; Silva-Tamayo et al., 2007). Calcium isotopic composition in archives that are relatively unaffected by seawater temperature potentially hold information about the changing chemical composition of the ocean water through time. This information is important as the chemical composition of the ocean itself is closely linked to the atmosphere and to the global climate. In order to reconstruct the calcium isotopic composition of the paleo-ocean archives such as brachiopods, belemnites, foraminifers, rudists, coccoliths, barites or phosphates are investigated (e.g., Nägler et al., 2000; Schmitt et al., 2003; Gussone et al., 2004; Fantle and DePaolo, 2005; Heuser et al., 2005; Immenhauser et al., 2005; Gussone et al., 2006; Hippler et al., 2006, 2009; Farkaš et al., 2007a,b; Sime et al., 2007; Griffith et al., 2008).

The biogenic calcite archive is prone to be affected by vital effects. Such vital effects are differentiated into either metabolic and kinetic

* Corresponding author. Present address: Section of Earth and Environmental Sciences, University of Geneva, Rue des Maraîchers 13, CH-1205 Geneva, Switzerland. Tel.: +41 22 379 66 20; fax: +41 22 379 32 10.
E-mail address: Elias.Samankassou@unige.ch (E. Samankassou).

effects (McConnaughey, 1989a,b) or into taxonomic and kinetic effects (Weiner and Dove, 2003). As an example, metabolic effects lower $\delta^{13}C$ via incorporation of respired CO_2 into foraminiferal tests (Spero and Lea, 1996; McConnaughey et al., 1997; Wilson-Finelli et al., 1998). Kinetic fractionation is linked to precipitation rate, i.e., fast precipitation leads to depletion of $\delta^{13}C$ and $\delta^{18}O$ in the shell. Accordingly, spawning, cold temperatures (depending on the species) and storms are thought to reduce growth rate of the brachiopod shell and, hence, increase the isotopic composition via kinetic fractionation. Taxonomic effects refer to an isotopic (disequilibrium) and/or elemental composition exerted by a phylum. Investigations regarding vital effects on calcium isotopes in skeletal carbonates have mainly focused on foraminifers, coccoliths, corals and bivalves (e.g., Skulan et al., 1997; Gussone et al., 2003; Immenhauser et al., 2005; Sime et al., 2005; Böhm et al., 2006; Gussone et al., 2007) whereas little is known about vital effects on calcium isotopes in brachiopods.

The calcium isotopic composition of inorganic carbonate precipitates (Gussone et al., 2003; Marriott et al., 2004) and of skeletal carbonates are positively correlated with temperature (e.g., Nägler et al., 2000; Gussone et al., 2003). As opposed to oxygen isotopes, calcium isotopes are more variable throughout abiogenic and biogenic calcite and are characterized by different slopes and offsets. Cultured and modern foraminifera such as *Globigerinoides sacculifer* show the steepest slopes of all with a temperature dependence of 0.24 and 0.22‰/°C, respectively (Nägler et al., 2000; Hippler et al., 2006) followed by the foraminifera *Neogloboquadrina pachyderma* (sin.) with 0.17‰/°C (Hippler et al., 2009). The foraminifera *Orbulina universa,* on the other hand, has a much lower slope of 0.019‰/°C which is very similar to experimental inorganic aragonite with 0.015‰/°C (Gussone et al., 2003). However, calcium isotope fractionation in foraminifers was found not to be solely dominated by temperature (Gussone et al., 2009). The coccolith *Emiliania huxleyi* has a temperature dependence comparable to that of *O. universa* with 0.027‰/°C (Gussone et al., 2006). The weak temperature dependence of about 0.02‰/°C suggested for certain inorganic and biogenic calcite includes brachiopods. Previous studies have established that calcium isotopic compositions of modern brachiopod shells are about 0.85‰ lighter than the $\delta^{44/40}Ca$ of the coeval seawater (Gussone et al., 2005; Farkaš et al., 2007a,b). Based on the assumption that this offset is valid for all modern and fossil brachiopods and remains constant through time, this value has been used to reconstruct the calcium isotopic evolution of the Phanerozoic (Farkaš et al., 2007a).

The aim of this study is to investigate, for the first time, intra-shell homogeneity and the reliability of modern-day brachiopods as an archive for the calcium isotopic signature of coeval seawater. In particular, the focus is on the species and temperature dependence of the calcium isotope fractionation, as well as the influence of seasonal variations of the growth environment. Additionally, we examine the record of ambient seawater temperatures by comparing oxygen and calcium isotopes along the profile of brachiopod shells with on-site measured seawater temperatures. Two modern brachiopod species, one that experienced variable seawater temperatures (*Terebratulina septentrionalis)* and one that lived at virtually constant temperatures (*Gryphus vitreus*) are examined for calcium, oxygen and carbon isotopic variations along the ontogenetic growth direction.

2. Material

The investigated modern brachiopods species *Terebratulina septentrionalis* (Couthouy) and *Gryphus vitreus* (Born) are both articulated, belonging to the order Terebratulida and the suborder Terebratulidina. They have entirely calcitic, endopunctate shells. The optimum growth temperatures for Terebratulida are between about 10 and 17 °C, although 2 and 28 °C mark the minimum and the maximum growth temperatures, respectively (Brand et al., 2003). *T. septentrionalis* shells were collected live in the spring of 1973 by Logan off the east side of Deer Island, New Brunswick, Bay of Fundy, Canada. The specimens normally live in shallow water at a depth of between 5–30 m (relative to mean low water), notwithstanding the high tidal range of 8.3 m at maximum. Water temperatures at nearby Letete Passage were 3.5, 5.6, 10.6, and 8.8 °C and salinities were 31.9, 30.9, 31.9, 32.1‰ for February, May, August and November, respectively (Shenton and Horton, 1973). The shell of *T. septentrionalis* is composed of two layers: an outer, thin, fine-grained primary layer and an inner, thicker, fibrous secondary layer (Fig. 1) (Williams 1968; Emig 1990). According to Emig (1990), *T. septentrionalis* normally extends from the subtidal down to about 1500 m depth globally but its greatest density along the east coast of Canada occurs on rocky subtidal substrates between 5 and 30 m (Logan and Noble, 1971; Noble et al., 1976).

Recent *G. vitreus* shells were collected live by Logan from dredge hauls in 1975 from the head of a submarine canyon (Canyon de Planier) off the southern coast of France near Marseille. The shells were located at a depth of around 200 m on gravelly substrates where water temperatures are constant with negligible variations between 12.7 and 13.6 °C and salinity variations between 38.10 and 38.50‰ (ranges from Medatlas data base [http://www.ifremer.fr/medar/] and Suivilion cruises data; personal communication, Xavier Durrieu de Madron, 2009). The shell of *G. vitreus* differs from that of *T. septentrionalis* in having three layers instead of two. The outermost primary layer is of a thin granular nature, followed by a thin fibrous secondary and a thick prismatic tertiary layer (Fig. 1). In peripheral areas of the shell the tertiary layer completely pinches out and the secondary layer becomes dominant (Williams 1968; MacKinnon and Williams, 1974; Benigni 1985; Gaspard 1986; Bitner and Moissette, 2003). *Gryphus vitreus* lives from the shelf break at 150 m to about 300 m depth (Emig 1987, 1989a,b).

3. Method

3.1. Shell preparation

Brachiopod shells were cleaned with distilled water only (except one *T. septentrionalis* which was additionally cleaned with Clorox) to avoid changes in shell chemistry. A toothbrush and a metal needle were used to remove dirt and superficial organic material. The ventral valves of *T. septentrionalis* (R1 + R2) and *G. vitreus* (R3) were cut in two halves along the growth direction with a Dremel® hand-drill equipped with a cut-off wheel. The thin outer primary layer was not removed. For isotopic analysis shell pieces of about 1.5 by 3–4 mm surface were sectioned from within the visible growth increments. This sampling method was chosen to investigate isotopic variations along the growth direction and to explore the effect of seasonal seawater temperature variations on the isotopic composition. The larger shell size of *G. vitreus* allowed additional sampling of pronounced growth lines (Fig. 1). Samples were ground with an agate mortar and split in two aliquots, one was used for $\delta^{44/40}Ca$ and the other for $\delta^{18}O$ and $\delta^{13}C$ analyses. The primary layer of *G. vitreus* (R3S.PL) was sampled by grinding off only the outermost part of the shell with the drill bit. One additional sample of *G. vitreus* (R4.1) was analyzed from a slightly smaller and, hence, younger specimen. Two remaining halves of the shells (R1 + R3) were prepared as 200 µm thick sections for in-situ chemical laser-ablation inductively-coupled-plasma mass-spectrometry (LA-ICP-MS) analysis.

3.2. Sample preparation and analytical methods

Calcium purification of *T. septentrionalis* samples followed Hippler et al. (2006). Remaining organic material was removed with a 1:4 H_2O_2–HNO_3 solution (Hippler et al., 2004). About 5 µg Ca was loaded on a single Ta filament with HCl and diluted H_3PO_4. The $\delta^{44/40}Ca$ ratio was measured on a modified single cup AVCO® thermal ionization mass spectrometer (TIMS) with a thermolinear source, at the

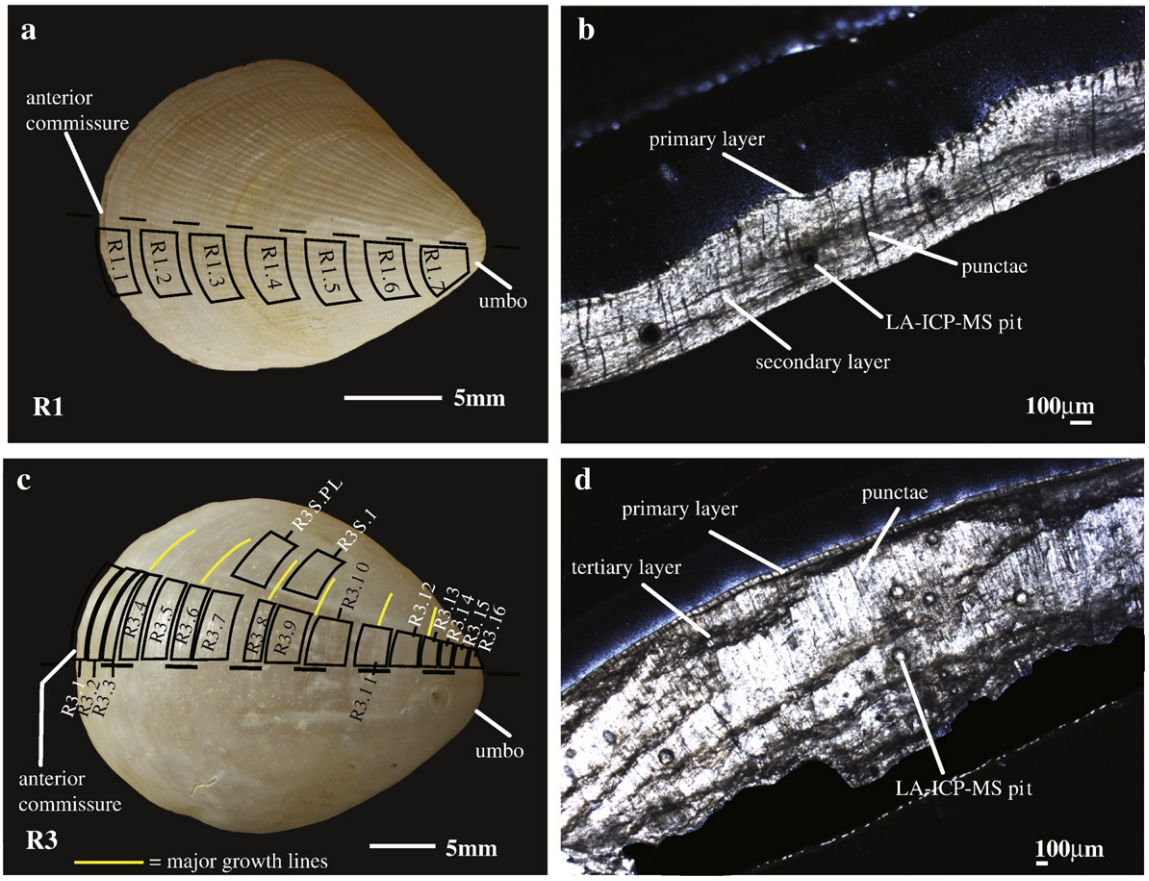

Fig. 1. Sample positions and 200 µm thin sections of *T. septentrionalis* (R1) (a,b) and *G. vitreus* (R3) (c,d). The umbo corresponds to the juvenile part of the shell whereas the anterior commissure corresponds to the terminal part of the shell. Microphotographs are taken in transmitted light. The outer primary layer is only about 20–40 µm in thickness. The secondary layer of *G. vitreus* cannot be distinguished in d.

University of Bern, Switzerland. The instrumentation setup corresponds to that described in Hippler et al. (2006). No isobaric interferences on masses 40, 43 and 44 from K^+ and Sr^{2+} (monitored masses 41 and 43.5, respectively) occurred at any time of the measurement. A ^{43}Ca–^{48}Ca double-spike technique was applied to correct for mass-dependent isotope fractionation in the TIMS. External reproducibility of the laboratory fluorite (CaF2) standard was better or equal to ±0.16‰ for *T. septentrionalis* and ±0.25‰ for *G. vitreus* (2σ standard deviation; $n=14$ and $n=8$ for *T. septentrionalis* and *G. vitreus*, respectively). The blank was less than 40 ng, which equals 0.8%.

Additional measurements of the *G. vitreus* shell were carried out at IFM-GEOMAR in Kiel, Germany following the method described in Heuser et al. (2002). The procedure was basically the same as in Bern. However, only 300 ng calcium were loaded on a Re filament with a Ta-based activator. The $\delta^{44/40}Ca$ composition was measured on a multicollector mass-spectrometer (Triton, ThermoFisher) in dynamic mode, using NIST SRM915a $CaCO_3$ standard material. ^{40}Ca intensities were mainly between 10 and 18 V during measurements. External precision is given as two times the standard error of the mean ($2SEM = 2\sigma/n^{0.5}$) determined by sample repeated sample measurements. The average precision for SRM915a during a session was ±0.092‰ 2SEM ($n=4$ per session, except once $n=3$). The $\delta^{44/40}Ca$ values for each session were calculated from the session mean of the SRM915a value. The blank is less than 16 ng, which is less than 5.4%. Results are expressed as $\delta^{44/40}Ca$ relative to NIST SRM915a using $\delta^{44/40}Ca = ((^{44}Ca/^{40}Ca)_{sample}/(^{44}Ca/^{40}Ca)_{standard} - 1) * 1000$ (Eisenhauer et al., 2004). $\delta^{44/40}Ca$ data from Bern, measured relative to the fluorite standard, were converted to NIST SRM915a by adding 1.47‰ (Hippler et al., 2003).

It seems that, in accordance with Farkaš et al. (2007a), there is a slight inter-laboratory difference of approximately 0.15‰. This difference is not related to scatter but to a systematic offset. During an inter-laboratory comparison, calcium isotopic data from Bern were in excellent agreement with the laboratories of Kiel and Strasbourg (Hippler et al., 2003). There is no obvious source for the observed offset. All results from Kiel were systematically increased by 0.15‰ to account for this bias.

$\delta^{18}O$ and $\delta^{13}C$ isotopes from aliquots of *T. septentrionalis* were measured at the University of Lausanne, Switzerland, using a Finnigan GasBench II with a carbonate auto-sampler linked to a Finnigan Delta^{Plus}XL mass spectrometer. The calcite powders (30–300 µg) reacted with 99% H_3PO_4, reaction time 4*18 min at 70 °C. Average standard reproducibility is 0.13 and 0.09‰ (1σ) for $\delta^{18}O$ and $\delta^{13}C$, respectively. O and C isotope measurements for *G. vitreus* were carried out at the University of Bern, Switzerland, using a GasBench II/Thermo Delta V Advantage. 150–200 µg calcite powder reacted with 100% H_3PO_4 for 82 min at 72 °C. Average long-term precision is 0.061 and 0.059‰ for $\delta^{18}O$ and $\delta^{13}C$, respectively ($n=435$, 1σ). All $\delta^{18}O$ and $\delta^{13}C$ data are expressed in ‰ relative to Vienna Peedee Belemnite (V-PDB). The $\delta^{18}O$ composition of the seawater ($\delta^{18}O_w$) was determined by entering the directly measured seawater salinities into the formula by Spero and Lea (1996), which was computed for northern and southern California surface waters between 1989 and 1993:

$$\delta^{18}O_w = 0.39*\text{salinity} - 13.46$$

Brand et al. (2003) tested other salinity-$\delta^{18}O_w$ formulae with a sample population and found that the results were within ±0.5 °C error of the Spero and Lea (1996) formula.

$\delta^{18}O$ values from the modern brachiopods ($\delta^{18}O_c$) were transformed into seawater temperatures by using the formula from Epstein et al. (1953).

$$T(^{\circ}C) = 16.5 - 4.3*(\delta^{18}O_c - \delta^{18}O_w) + 0.14*(\delta^{18}O_c - \delta^{18}O_w)^2$$

Elemental contents were analyzed by LA-ICP-MS at the University of Bern, Switzerland. The equipment consists of a GeoLas-Pro 2006, 193 nm wavelength, ArF Excimer laser system (Lambda Physik/Coherent) combined with an Elan DRC-e quadrupole mass-spectrometer (Perkin Elmer) and was run at conditions similar to those reported in Pettke (2008). CaO served as an internal standard and NIST SRM610 was used for external standard calibration. Background was measured for about 50 s and average signal acquisition time was around 30 s. Sample beam sizes varied between 24 and 120 μm whereas SRM610 beam size was 44 μm. All data were processed using the LAMTRACE data reduction program (Jackson, 2008). The external analytical reproducibility is routinely better than 3%. Point analyses were acquired along the longitudinal shell section, as depth profiles and in the primary layer of the ventral valves.

Strontium concentrations of two additional *Gryphus vitreus* samples, R3S.1 and R4.1, were analyzed by inductively coupled plasma atomic emission spectroscopy (ICP-AES) at the Laurentian University, Sudbury, Canada. About 10 mg of powdered sample were dissolved in PTFE beakers in a mixture of concentrated HF (0.5 ml) and HNO_3 (0.25 ml) for 72 h at 140 °C. After evaporation samples were converted twice in concentrated HNO_3, centrifuged and then diluted to 2% HNO_3 for ICP measurements. USGS standards BHVO-2 and BIR-1d were used for standardization. The 3-year long-term external reproducibility is better than 1% for most elements. The relative standard deviation for Sr is 1.1%.

4. Results

4.1. Elemental composition and textural preservation

Elemental composition of the secondary layer of *T. septentrionalis* (R1) and the tertiary layer of *G. vitreus* (R3) plot entirely within published data of modern brachiopods (Brand 1989; Brand et al., 2003) except the Mn content of the secondary and especially the tertiary layer of *Gryphus vitreus* which is an order of magnitude smaller (Table 1). Small specimen-specific elemental deviations from Brand et al. (2003) can readily be explained by the small sample size of the LA-ICP-MS method. Transmitted light microscopy revealed excellent preservation of the shells and the presence of the primary and secondary layer in R1 and the primary, secondary and tertiary layer in R3.

4.2. Calcium isotopes

Intra-shell $\delta^{44/40}Ca$ values of *T. septentrionalis* range from 1.00 to 1.16‰ for R1 and from 0.84 to 1.13‰ for R2 (Table 2, Fig. 2a and b). The five $\delta^{44/40}Ca$ data points per shell suggest a negative correlation with oxygen isotopes of $r = -0.70$ and $r = -0.93$ for both R1 and R2, respectively (Table 3) and a negative correlation with carbon isotopes with $r = -0.81$ and $r = -0.71$, respectively. In spite of the apparent negative correlation calcium data are not significantly different from each other given the analytical error. Furthermore, only the correlation between calcium and oxygen isotopes of R2 is statistically significant with a p-value of 0.02 (using Soper, 2009, Table 3). The average $\delta^{44/40}Ca$ values of R1 and R2 are within statistical uncertainty identical with 1.08 and 1.02‰, respectively, which is approximately 0.80‰ lighter than seawater. Neither umbonal nor anterior commissural areas of the shell show any significant deviation from the average.

Calcium isotopes of R3 range from 1.13 to 1.46‰ (this includes Bern and Kiel data), which is comparable to the range of R2 (Table 2). The average $\delta^{44/40}Ca$ value of R3 of 1.32‰ is only 0.56‰ lighter than seawater. This is slightly different from the results of *T. septentrionalis*. R3 calcium isotopes show no significant correlation with $\delta^{18}O$ and $\delta^{13}C$ (Table 3, Fig. 2c). No influence of major growth lines on calcium isotopes could be detected (Table 2). Calcium isotopic values of R3 are heaviest in the central part of the transect and trend towards lighter values near the marginal parts approaching maximum isotopic composition of *T. septentrionalis*. Two additional samples of R3 were analyzed (Table 4). R3S.1 is situated at about the same distance along the ontogenetic transect as R3.9 but is laterally offset towards where growth increments are smaller and the shell of *G. vitreus* is thicker (Fig. 1). The result of R3S.1 of 1.35‰ agrees well with the average $\delta^{44/40}Ca$ of R3 of 1.32‰ and with its lateral counterpart R3.9 of 1.30 and 1.35‰. The 1.04‰ of the primary layer (R3S.PL) of *G. vitreus* is slightly lighter than the average. The R4.1 sample from a different, slightly smaller, *G. vitreus* specimen is with 1.23‰ close to the average of R3 (Tables 2 and 4). The R4.1 location in the shell is comparable to R3S.1.

4.3. Oxygen and carbon isotopes

$\delta^{18}O$ values of the two investigated valves of *T. septentrionalis* range from 0.6 to 1.1‰ for R1 and from 0.5 to 1.3‰ for R2. The corresponding $\delta^{13}C$ values range from 1.6 to 2‰ and from 1 to 1.6‰, respectively (Table 2). The $\delta^{18}O$ range of *T. septentrionalis* is about 3 times the range of calcium isotopes. When plotting $\delta^{18}O$ versus $\delta^{13}C$, R1 and R2 do not display any statistically significant correlation (Table 3) with p-values of 0.9 and 0.3, respectively. However, a similar $\delta^{18}O$ and $\delta^{13}C$ trend can be observed along the growth direction of the R2 shell (Fig. 2b). $\delta^{18}O$-derived temperatures range from 7.0 to 10.7 °C for R1 and from 6.2 to 11.2 °C for R2 (Table 5) whereas temperatures measured on-site vary between 3.5 and 10.6 °C. The calculated ranges of 3.7° and 5.0 °C are smaller than the on-site measured range of 7.1 °C. Calculated average temperatures of 8.7 and 8.6 °C for R1 and R2, respectively, lead to an overestimation of about 1.6 °C of the actual mean seawater temperature of 7.1 °C.

Table 1
LA-ICP-MS data of *T. septentrionalis* (R1) and *G. vitreus* (R3) in ppm.

	Sr		Na		Mg		Mn		Fe	
	Min	Max	Min	Max	Min	Max	Min	Max	Min	Max
T. septentrionalis Primary layer ($n = 8$)	1690	2100	4150	5300	4300	9400	1.9	13.2	<15.4	41.0
T. septentrionalis Secondary layer ($n = 34$)	980	1420	2570	3650	1700	5300	4.5	16.9	3.9	11.0
Gryphus vitreus Primary layer ($n = 2$)	1520	1670	4250	4800	4170	5980	<0.8	2.1	<11.8	12.2
Gryphus vitreus Secondary layer ($n = 5$)	970	1180	2401	3554	1723	2433	5.7	6.9	7.8	11.9
Gryphus vitreus Tertiary layer ($n = 22$)	480	650	550	1200	440	3000	0.07	0.9	<4	9.8

Table 2
Isotope results: *T. septentrionalis* (R1 and R2) and *G. vitreus* (R3) in per mil.

	R1				R2				R3[a,b]					
Sample	$\delta^{44/40}$Ca	Error[c], (*n*)	δ^{18}O	δ^{13}C	$\delta^{44/40}$Ca	Error[c], (*n*)	δ^{18}O	δ^{13}C	$\delta^{44/40}$Ca	Error[c], (*n*)	$\delta^{44/40}$Ca	Error[c], (*n*)	δ^{18}O	δ^{13}C
Rx.1	1.12	±0.04 (1)	0.60	1.78			0.85	1.59					2.29	2.11
Rx.2			0.66	1.77	1.12	±0.04 (1)	0.51	1.38			1.13	±0.07 (2)	2.12	2.31
Rx.3	1.00	±0.05 (1)	0.99	2.04	1.05	±0.05 (1)	0.47	1.31					2.36	2.55
Rx.4	1.02	±0.04 (1)	1.11	1.80			1.22	1.47	1.45	±0.06 (1)			2.45	2.67
Rx.5	1.16	±0.10 (1)	0.88	1.68	0.84	±0.05 (1)	1.23	1.55	1.35	±0.06 (1)			2.37	2.90
Rx.6			1.02	1.61	0.94	±0.04 (1)	0.97	1.30	*1.29*	*±0.13 (3)*			2.44	3.12
Rx.7	1.11	±0.06 (1)	0.82	1.79	1.13	±0.05 (1)	0.59	1.06	*1.30*	*±0.20 (3)*			2.37	3.08
Rx.8							1.33	1.50	*1.27*	*±0.15 (3)*			2.39	3.26
Rx.9							0.98	1.02	*1.30*	*±0.05 (3)*	1.35	±0.08 (1)	2.35	3.11
Rx.10									*1.33*	*±0.03 (3)*	1.46	±0.08 (1)	2.20	3.05
Rx.11									*1.44*	*±0.20 (3)*			2.16	3.01
Rx.12									*1.14*	*±0.07 (3)*	1.39	±0.31 (3)	2.10	2.90
Rx.13									*1.20*	*±0.09 (3)*			2.07	2.78
Rx.14													2.10	2.77
Rx.15													2.15	2.62
Rx.16													2.18	2.58
Min	1.00		0.60	1.61	0.84		0.47	1.02	1.13				2.07	2.11
Max	1.16		1.11	2.04	1.13		1.33	1.59	1.46				2.45	3.26
Average	1.08		0.87	1.78	1.02		0.91	1.35	1.32				2.26	2.80
Range	0.16		0.50	0.43	0.29		0.85	0.57	0.33				0.38	1.15

$\delta^{44/40}$Ca is given relative to NIST SRM915a; δ^{18}O and δ^{13}C are relative to V-PDB.
[a] $\delta^{44/40}$Ca from Kiel are in italics.
[b] Kiel data are shifted by +0.15‰ to correct for the inter-laboratory offset.
[c] $\delta^{44/40}$Ca errors are given as 2SD for $n = 1$ and as 2SEM for $n > 1$, 2σ external standard reproducibility for R1 and R2 is better or equal to ±0.16‰, for R3 (Bern data) ±0.25‰ and for R3 (Kiel data) ±0.092‰ (session mean), (*n*) denotes number of repeat measurements, major growth lines of R3 are underlined.

The δ^{18}O values of *G. vitreus* show little variability, ranging from 2.1 to 2.5‰, whereas δ^{13}C values display a wide range between 2.1 and 3.3‰ (Table 2). All samples cut along the ontogenetic growth direction are included in these ranges. The δ^{18}O range of *G. vitreus* is comparable to the calcium isotopic range. There is no statistically significant correlation between δ^{18}O and δ^{13}C values with the p-value at 0.29 (Table 3). The δ^{18}O-derived temperature range of 2.1 °C exceeds the measured range by 1.2 °C. The δ^{18}O-derived average temperature of 13.6 °C compares well with the measured 13.1 °C (Table 5). Carbon isotopes are lighter towards the umbonal and anterior commissural part of *G. vitreus* than in the center of the shell.

5. Interpretation and discussion

5.1. Calcium isotopes

The small $\delta^{44/40}$Ca ranges of 0.16, 0.29‰ (R1 and R2, respectively) recorded along the ontogenetic growth direction in modern ventral valves of *T. septentrionalis* are within external reproducibility (±0.16‰ for R1 and R2). Hence, calcium isotopes are fractionated homogeneously along the median line of the ventral shell of the investigated *T. septentrionalis* specimen given the above-described measurement precision. The results from R1 suggest that growth rate does not influence calcium isotope fractionation in *T. septentrionalis* as the umbonal and anterior commissural parts of the shell, where growth is thought to be fastest and slowest, respectively, are close to the average isotopic composition (Fig. 2a). The calcium isotopic range along the ontogenetic growth direction of *G. vitreus* is comparable to *T. septentrionalis* with 0.33‰. Unlike *T. septentrionalis*, $\delta^{44/40}$Ca values in the *G. vitreus* shell become somewhat lighter towards umbo (R3.12 & R3.13) and anterior commissure (R3.2). In the marginal area of R3.2 the tertiary layer is almost absent and the secondary layer increases in thickness. The relatively light value of R3.2 of 1.13‰ is influenced by the larger portion that the primary layer (1.04‰, R3S.PL) occupies in this thin shell area. It is also likely that the secondary layer has a lighter calcium isotopic composition than the average shell value of 1.32‰. This may either be caused by a signature inherent to the secondary layer or by vital effects in the marginal shell part. The trend towards light values in the umbonal region of *G. vitreus* (R3.12 and R3.13) is not caused by a possible light signature of the secondary layer as this layer is only dominant at the very peripheral part of the umbo. The umbonal position of R3.12 and R3.13 might suggest kinetic fractionation due to fast growth rate during the juvenile stage of the shell. However, a fast growth rate should lead to depletion in carbon and oxygen isotopes. Fig. 2c shows a negative trend in oxygen isotopes of the first four juvenile samples (R3.16 to R3.13) but carbon isotopes do not follow this trend; instead a negative correlation with oxygen is apparent in this portion of the shell. Thus the hypothesis of light calcium isotopes in the umbonal area due to fast growth rates is not supported. Other possible differences in growth rate along the shell of *G. vitreus* cannot be distinguished since $\delta^{44/40}$Ca results between growth increments ('fast' growth rate) and growth lines ('slow' growth rate) are indistinguishable (Fig. 2c, Table 2). However, the sampling method may average out a possible growth rate effect as the shell not only is accreted at the terminal part but also thickness is constantly increased during the life of a brachiopod. It has to be noted that *G. vitreus* grew under virtually constant temperature and salinity conditions, which is thought to lead to a constant growth mode with the exception of, for instance, spawning which presumably slows down growth.

The indicated opposite behavior of δ^{18}O and $\delta^{44/40}$Ca (Fig. 2a and b) possibly points to a small seasonal temperature-dependent Ca isotope fractionation – maybe driven by metabolism – in *T. septentrionalis*. Being aware of the limited analytical resolution in $\delta^{44/40}$Ca and the fact that only the correlation coefficient of R2 is statistically significant (Table 3), we nevertheless calculated $\delta^{44/40}$Ca-temperature variations within the shell of *T. septentrionalis* by using the on-site measured temperature range. This yields a temperature gradient of 0.02 and 0.04‰/°C, respectively, for R1 and R2. If the same calculation is done using the δ^{18}O-derived temperature range, then R1 and R2 result into a temperature gradient of 0.04 and 0.06‰/°C, respectively. Contrary to oxygen isotopes, the $\delta^{44/40}$Ca range of the *G. vitreus* shell (constant temperature) is comparable to the $\delta^{44/40}$Ca range of *T. septentrionalis* that experienced 7.1° temperature variations.

Fig. 3 shows this study's isotopic data and brachiopod data from Gussone et al. (2005) plotted against temperature. All depicted brachiopods consist of a low Mg calcite shell. Brachiopod data from Gussone et al. (2005) suggest a weak $\delta^{44/40}$Ca-temperature

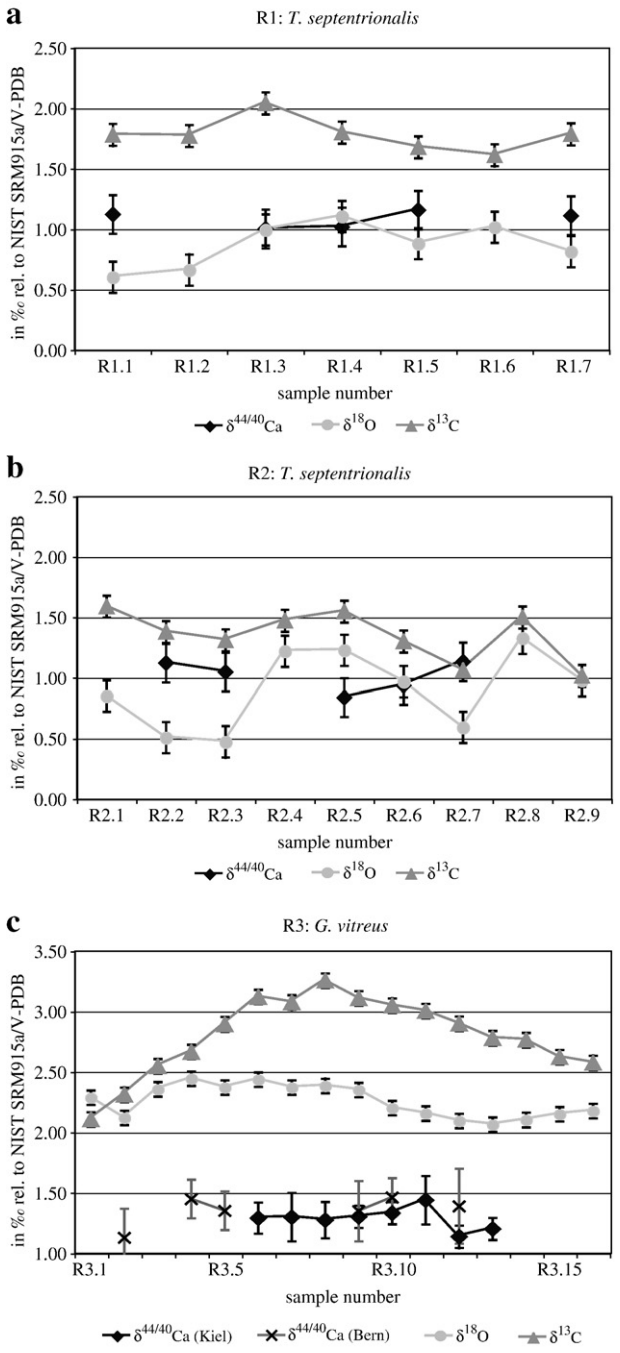

Fig. 2. Isotopic results along the ontogenetic growth direction. Samples Rx.1 are located at the terminal part of the shell (commissure, see Fig. 1). Note the shifted – but range conserving – scale of the *Y*-axis in c. Error bars denote the 1σ average standard long-term precision for O and C isotopes. Ca isotope errors are given as 2σ standard deviation of the external reproducibility or as repeat sample error (2SEM) if this exceeds the former.

Table 3
Correlation coefficient r and *p*-values (two-tailed) (*r*/*p*).

	R1		R2		R3	
	$\delta^{18}O$	$\delta^{13}C$	$\delta^{18}O$	$\delta^{13}C$	$\delta^{18}O$	$\delta^{13}C$
$\delta^{44/40}Ca$	−0.70/0.19	−0.81/0.10	−0.93/0.02	−0.71/0.18	0.55/0.08	0.32/0.34[a]
$\delta^{18}O$		0.08/0.86		0.42/0.27		0.28/0.29

p-values are calculated using the application of Soper, 2009.
[a] Includes all Kiel data and R3.2, R3.4 and R3.5 from Bern.

Table 4
Additional samples from *G. vitreus*.

Sample	$\delta^{44/40}Ca$	Error[a], (n)	$\delta^{18}O$	$\delta^{13}C$	Sr (ppm)
R3S.1	1.35	±0.07 (1)	2.34	2.97	535
R3S.PL	1.04	±0.22 (3)	–	–	~1595
R4.1	1.23	±0.10 (1)	2.34	2.95	606

$\delta^{44/40}Ca$ is given relative to NIST SRM915a; $\delta^{18}O$ and $\delta^{13}C$ are relative to V-PDB.
[a] $\delta^{44/40}Ca$ errors are given as 2SD for $n=1$ and as 2SEM for $n>1$, 2σ external standard reproducibility is better or equal to ±0.25‰, the Sr value for sample R3S.PL is an estimated average from LA-ICP-MS data (Table1), (*n*) denotes number of repeat measurements.

dependence of about 0.015‰/°C. Apparently *G. vitreus* does not reflect temperature in its calcium isotopes when compared to the brachiopod temperature gradient of Gussone et al. (2005). However, the $\delta^{18}O$-temperature calculations of *G. vitreus* agree with on-site measured seawater temperatures. The trendline through the *T. septentrionalis* data in Fig. 3 indicates that a potential temperature correlation of *T. septentrionalis* would not extend to published whole-shell data from other species (Gussone et al., 2005), supporting species-specific processes. As opposed to the species measured by Gussone et al. (2005), and many other two-layered brachiopod shells, *G. vitreus* secretes an additional thick tertiary prismatic layer. Maybe this physiological difference results in a heavier $\delta^{44/40}Ca$ species-specific isotopic composition of *G. vitreus*. *Thecidellina* sp., the brachiopod species that is mainly responsible for the 0.015‰ temperature gradient derived from the Gussone et al. (2005) data, also has a specific shell structure. It is composed predominantly of primary layer calcite (Williams, 1973). If there is such a species-specific isotopic calcium composition in brachiopods with specialized shell structures then these specimens should not be used to determine the temperature gradient for brachiopods. Ideally, a temperature gradient should be tested among a single species or at least within the same order.

Tang et al. (2008) detected a positive correlation between calcium isotope fractionation and strontium content in experimental inorganic calcite precipitated from an experimental fluid close to seawater and, with a significantly lower slope, in the Phanerozoic brachiopods studied by Farkaš et al. (2007a) (Fig. 4). The slope of experimental inorganic calcite was found to be related to the kinetic effects of precipitation rates and temperature (Tang et al., 2008). The slope of fossil Phanerozoic brachiopods was suggested to mirror the Sr and $\delta^{44/40}Ca$ composition of coeval seawater rather than kinetics of $CaCO_3$ crystallization (Tang et al., 2008) and, hence, might be driven by the changing aragonitic versus calcitic ocean chemistry (Steuber and Veizer, 2002; Farkaš et al. 2007a). However, Tang et al. (2008) pointed out that the experimental fluid solution did not contain Mg and, hence, might not be directly comparable to seawater and its precipitates. The three modern brachiopods measured by Steuber and Buhl (2006) and Farkaš et al. (2007b) plot close together near the experimental slope (Fig. 4). The present study's average $\delta^{44/40}Ca$ of *T. septentrionalis* is slightly heavier than predicted by the experimental inorganic calcite formula of Tang et al. (2008). Nevertheless the average of *T. septentrionalis* (R1) plots close to the three modern

Table 5
Measured and $\delta^{18}O$-derived seawater temperatures for *T. septentrionalis* (R1 and R2) and *G. vitreus* (R3) in °C.

	R1 calculated	R2 calculated	R1&R2 measured	R3 calculated	R3 measured
Min *T*(°C)[a]	7.0	6.2	3.5	12.6	12.7
Max *T*(°C)[a]	10.7	11.2	10.6	14.7	13.6
Range (°C)	3.7	5.0	7.1	2.1	0.9
Average (°C)	8.7	8.6	7.1	13.6	13.1

[a] 30.91 and 32.14‰ were used as min and max salinity for R1 and R2 $\delta^{18}O$ temperature calculations, 38.10 and 38.50‰ were used for R3.

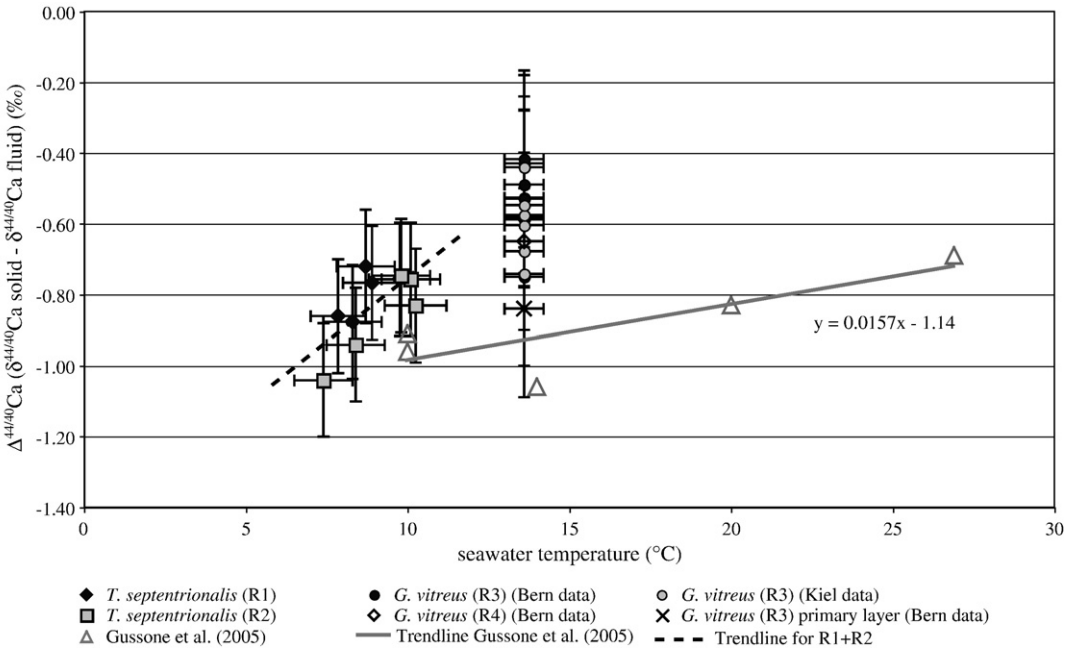

Fig. 3. Trendline through modern brachiopod data from Gussone et al. (2005) compared with *T. septentrionalis* (R1 + R2) and *G. vitreus* (R3 + R4) versus temperature. Data are given relative to seawater as $\delta^{44/40}$Ca ($\delta^{44/40}$Ca solid − $\delta^{44/40}$Ca fluid). $\delta^{44/40}$Ca values of *T. septentrionalis* and *G. vitreus* are plotted at the average of the corresponding calculated δ^{18}O-seawater temperature. Maximum and minimum $\delta^{44/40}$Ca values do not always correspond with maximum and minimum δ^{18}O values. The temperature error bars delimit the calculated δ^{18}O temperatures for the entire measured salinity range. Error bars give the 2σ external reproducibility of the Bern data.

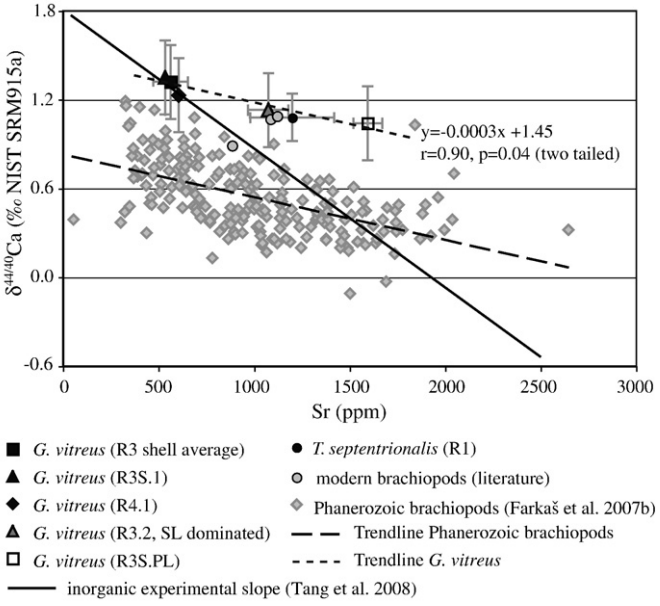

Fig. 4. The $\delta^{44/40}$Ca vs Sr (ppm) plot, including data from this study and literature (Steuber and Buhl, 2006; Farkaš et al., 2007b), shows that modern brachiopods plot relatively close to the kinetically driven inorganic experimental slope from Tang et al. (2008). SL = secondary layer, PL = primary layer. The samples of *G. vitreus* that deviate most from the experimental slope are the primary layer (R3S.PL) and the sample that is dominated by secondary layer (R3.2). A hypothetical trendline through all data from *G. vitreus* ($r = 0.90$, $p = 0.04$, two tailed) is similar in slope to the trendline of Phanerozoic brachiopods (Farkaš et al., 2007a), which are thought to mirror ambient seawater composition (Tang et al., 2008). The point where the hypothetical trendline through the data from *G. vitreus* crosses the experimental line may indicate slow equilibrium fractionation of most of the samples from *G. vitreus*. With the exception of R3S.1 and R4.1, the arithmetic mean of the maximum and minimum LA-ICP-MS data is used to plot Sr whereas the min. and max. Sr contents are given as error bars. For R3 (transect values), R3.2 and R3S.PL, LA-ICP-MS data from the tertiary, secondary and primary layer are used, respectively. The error bars of R3S.1 and R4.1 depict the 1.1 rsd of ICP-AES analyses. $\delta^{44/40}$Ca error bars are given as 2σ external reproducibility from Bern (modified after Tang et al. 2008).

brachiopods from Steuber and Buhl (2006) and Farkaš et al. (2007b). The average of *G. vitreus* (R3) and the additional *G. vitreus* samples R3S.1 and R4.1, however, have lower Sr contents and higher $\delta^{44/40}$Ca values than *T. septentrionalis* and the modern brachiopods from Steuber and Buhl (2006) and Farkaš et al. (2007b). Nevertheless, these *G. vitreus* samples plot very close to the experimental inorganic calcite slope (Fig. 4).

The somewhat particular isotopic and elemental composition of *G. vitreus* cannot be explained by variation in seawater composition since strontium and magnesium have a long residence time. These elements are homogeneously distributed throughout the ocean, except for minor local variations in salinity in connection with freshwater-seawater mixing (Wolf et al., 1967; Klein et al., 1996a; Klein et al., 1996b). The elevated salinity of the Mediterranean Sea might be expected to lead to a slightly higher Sr and Mg shell composition but this does not fit the low trace elemental contents of *G. vitreus*. Moreover, the present day $\delta^{44/40}$Ca-signature of the ocean is considered to be homogeneous within analytical uncertainties (Zhu and MacDougall, 1998; De La Rocha and DePaolo, 2000; Schmitt et al., 2001). Obviously *G. vitreus* shows a distinct lower concentration of trace elements than other species. The specific calcium isotopic composition and Sr content of *G. vitreus* may be linked to the secretion of a specialized shell structure, i.e., the tertiary layer. On the other hand, a taxonomic difference in elemental composition has been suggested by the significantly higher overall level of Mg observed in *Terebratulina unguicula* compared with *Terebratalia transversa* valves (Buening and Carlson, 1992). Further studies such as, e.g., Popp et al. (1986), Grossman et al. (1996) and Buening et al. (1998) have proposed taxonomic effects on isotopic and elemental composition of brachiopods. The low Sr content and heavy calcium isotopic signature suggest that the tertiary layer of *G. vitreus* was secreted more slowly, i.e., close to equilibrium with seawater (either due to taxonomic effects or in relation to the specialized shell structure) than the secondary layers of *G. vitreus*, *T. septentrionalis* and other species with higher Sr and lighter calcium isotopic values (Steuber and Buhl, 2006; Farkaš et al., 2007b). The hypothesis of equilibrium precipitation of calcium isotopes in the tertiary layer of *G. vitreus* is further supported

as the mean values of *G. vitreus* plot on the experimental slope of Tang et al. (2008) whereas the primary layer (R3S.PL) and the sample dominated by the secondary layer (R3.2) somewhat deviate from the experimental slope. Interestingly, the indicated trendline of the samples of *G. vitreus* (Fig. 4; $r = 0.90$, $p = 0.04$, two tailed) is similar to, although offset from, the slope of the trend noticed by Tang et al. (2008) in Phanerozoic brachiopods (Farkaš et al., 2007a). Considering the low Sr concentration of *G. vitreus* and the positive correlation between calcium isotope fractionation and strontium content reported in Tang et al. (2008), as well as the variations of Sr content in modern brachiopods within the same order (Brand et al., 2003), care should be taken of possible species-specific calcium isotopic composition of brachiopods. The mean ontogenetic calcium isotopic value of *G. vitreus* is heavier than the commonly used 0.85‰ offset between the heavier seawater and the lighter brachiopods. However, the results from this study tentatively suggest that brachiopods with low Sr content might be closer to equilibrium with seawater than species with higher Sr content (Fig. 4). Hence, brachiopods with low Sr content such as *G. vitreus* might be more reliable carriers of the seawater signature than species with a higher Sr content. Additionally, the offset between seawater and brachiopods of −0.85‰ used for Phanerozoic seawater reconstructions may not be applicable for the entire Phanerozoic as the fractionation factor of brachiopod shells might be influenced by evolutionary trends in the brachiopod phylum.

A comparison between the intra-shell $\delta^{44/40}$Ca variations of 0.16 to 0.33‰ of both species and the suggested ~0.7‰ gradual increase of the seawater composition from the Ordovician to present (Farkaš et al., 2007a) leads to the conclusion that intra-shell variations may hamper ocean reconstructions. Furthermore, little is known about metabolic and taxonomic effects on calcium isotopic fractionation during biomineralization. Therefore, the average calcium isotopic inter-species differences of 0.24 to 0.30‰ between *T. septentrionalis* and *G. vitreus* and the indicated species-specific Sr content which may influence the calcium isotopic composition need further investigation. They might be responsible for some of the uniform ±0.25‰ scatter of the Phanerozoic seawater reconstruction based on brachiopods that Farkaš et al. (2007a) ascribed to a) measurement precision, b) temperature effect on calcium isotopes, c) minor enrichment of radiogenic ^{40}Ca, and d) diagenetic alteration. It should be noted that even with relatively large sample amounts, as used in this study from mid-shell areas of different brachiopod species, calcium isotopic values of coeval brachiopods can vary up to 0.62‰ (e.g., R3.10 versus R2.5, Table 2). This would clearly affect a calcium isotopic reconstruction of the paleo-seawater based on brachiopod shells.

5.2. Oxygen and carbon isotopes

δ^{18}O-derived average temperatures of this study from *T. septentrionalis* overestimate the on-site measured mean temperature by approximately 1.6 °C (Table 5). Due to the sampling strategy, i.e., "large" sample size and the omission of growth lines, absolute minimum and especially maximum δ^{18}O values were either attenuated or not sampled. The inclusion of the thin primary layer, which, according to Carpenter and Lohmann (1995), is very negatively fractionated in *T. septentrionalis*, may be partly responsible for this overestimation of temperature. In accordance with Carpenter and Lohmann (1995) and with Brand et al. (2003), *T. septentrionalis* is close to or within abiogenic oxygen isotopic equilibrium with the ambient seawater. δ^{18}O-derived temperatures of *G. vitreus* faithfully reflect ambient mean seawater temperatures (Table 5). The overestimation of the temperature range is likely to be caused by vital effects. Many authors have questioned the assumption that δ^{18}O values of brachiopod shells are in equilibrium with ambient seawater, because a biogenetically secreted calcite, prone to vital effects, cannot be compared to the precipitation of abiogenic calcite. In the present case of *T. septentrionalis* and *G. vitreus*, however, δ^{18}O values appear to reflect equilibrium with ambient seawater.

Interpretation of δ^{13}C values and trends of modern organic calcite is complicated by the multiple factors and processes that can influence δ^{13}C values of the habitat of the organism such as, e.g., geographic gradients, changes in productivity, upwelling, oxidation of organic matter or dissolution of aragonite. Furthermore, the life mode of the organism itself — epifaunal versus infaunal, water depth and metabolism will also influence the δ^{13}C of the shell, among other factors (Immenhauser et al., 2002, 2008 and references therein). In fossil material the interpretation of δ^{13}C is further complicated by late diagenetic alteration.

δ^{13}C ranges of *T. septentrionalis* are generally lower than δ^{18}O ranges (Table 2). Opposed to δ^{18}O there is an offset of about 0.40‰ between the average δ^{13}C of the two specimens. Since both specimens were collected from the same location only differences in microhabitat, metabolic or kinetic effects are thought to cause this offset. Interestingly the constant temperature *G. vitreus* shell shows a δ^{13}C range exceeding its δ^{18}O range by a factor of about 3 (Table 2). Furthermore, the δ^{13}C range is about twice the size of the δ^{13}C range of *T. septentrionalis.* Kinetic effects are not thought to be responsible for the large range of δ^{13}C since there is no correlation between δ^{13}C and δ^{18}O (Table 3). This may indicate that δ^{13}C variations of *G. vitreus* are influenced by metabolic effects or by fluctuating δ^{13}C values of the ambient seawater. Parkinson et al. (2005) noted that carbon isotopes were more variable throughout the secondary layer of brachiopods compared to oxygen isotopes and they showed no relation to the latter. These authors found low δ^{13}C values near the umbonal part of the shell in terebratulid and rhynchonellid brachiopods, which agree with the results of the present study. However, R1 and especially R3 do not fit Parkinson et al.'s (2005) findings of high δ^{13}C values towards the terminal part of the shell. Carbon isotopes are thought to increase towards the terminal part of calcifying marine organisms, due to lower growth rate with progressing age (e.g., Romanek and Grossman, 1989; Carpenter and Lohmann, 1995). Only R2 shows a possible slight age/low growth rate effect on carbon isotopes in its terminal part whereas R3 gets unexpectedly light towards the anterior commissure. This study's δ^{13}C results are in agreement with those obtained by Mii and Grossman (1994). These authors could not find a clear δ^{13}C pattern relative to shell growth in the shell of the Pennsylvanian brachiopod *Neospirifer dunbari* whereas equal δ^{18}O values paralleling growth bands were detected and interpreted as a temperature signal. In order to be able to accurately interpret large δ^{13}C variations such as in R3, close monitoring of the δ^{13}C fluctuations of the ambient seawater of the habitat would be required.

6. Conclusion

The small, up to 0.33‰, intra-specimen $\delta^{44/40}$Ca variations along the ontogenetic growth direction within the investigated modern brachiopod species *T. septentrionalis* and *G. vitreus* suggest that calcium isotopes are more homogenously distributed along the shell than oxygen and carbon isotopes. However, as shown in this study, difficulties for reconstructing the $\delta^{44/40}$Ca composition of the paleo-ocean may arise from using different brachiopod species, as the largest isotopic difference between mid-transect samples of *T. septentrionalis* and *G. vitreus* reaches 0.62‰. This isotopic difference may be species-dependent, likely upon Sr and/or Mg concentration or it may be related to the specialized shell structure of the tertiary layer of *G. vitreus*. Additionally, it is unknown whether the offset between seawater and brachiopods of −0.85‰ used for Phanerozoic seawater has remained unchanged during the long evolutionary history of brachiopods. These issues need further investigation before brachiopods can be used as reliable carriers of the ancient ocean $\delta^{44/40}$Ca composition.

The opposite behavior of δ^{18}O and $\delta^{44/40}$Ca in the *T. septentrionalis* shell may point to a possible seasonal temperature-dependent calcium

isotope fractionation; however, this issue remains unresolved. Smaller sample size and higher measurement precision would be required for further investigation of a possible recorded seasonal temperature signal. However, the Ca isotopic range from the constant temperature shell *G. vitreus* is comparable to the range of *T. septentrionalis*. This indicates that vital effects interfere with presumed small intra-specimen temperature signals.

$\delta^{18}O$ variations of *T. septentrionalis* and *G. vitreus* appear to be driven by temperature to some extent as $\delta^{18}O$-derived average temperatures are close to mean seawater temperatures measured on-site. Due to the sampling method and the inclusion of primary layer, $\delta^{18}O$-derived seasonal minimum temperatures are not entirely consistent with measured minimum temperatures. However, any thermodynamic fractionation in biogenic calcite seems to be influenced by vital effects and we still lack detailed knowledge of the extent and mechanism of these vital effects.

Acknowledgments

We kindly thank two anonymous reviewers for their much appreciated comments and input. Furthermore, we kindly acknowledge the editor J.D. Blum for handling our manuscript. P. Dietsche (University of Fribourg) is acknowledged for sample preparation. A. Kolevica (Leibniz-Institute of Marine Sciences, IFM-GEOMAR) and K. Howald (University of Bern) are acknowledged for technical support. Xavier Durrieu de Madron (CEFREM CNRS-UPVD, Perpignan) is acknowledged for providing precious temperature and salinity data for the Mediterranean Sea. This study was founded by the Swiss National Science Foundation (grant 200021-107505) and by the University of Fribourg.

References

Benigni, C., 1985. Morphologia ed ultrastruttura di *Gryphus vitreus* (Born, 1778) dell'Arcipelago Toscano (Italia). Boll. Mus. Reg. Sci. Nat. Torino 3, 449–498.

Bitner, M.A., Moissette, P., 2003. Pliocene brachiopods from the north-western Africa. Geodiversitas 25, 463–479.

Böhm, F., Gussone, N., Eisenhauer, A., Dullo, W.C., Reynaud, S., Paytan, A., 2006. Calcium isotope fractionation in modern scleractinian corals. Geochim. Cosmochim. Acta 70, 4452–4462.

Brand, U., 1989. Biogeochemistry of Late Paleozoic North American brachiopods and secular variation of seawater composition. Biogeochemistry 7, 159–193.

Brand, U., Logan, A., Hiller, N., Richardson, J., 2003. Geochemistry of modern brachiopods: applications and implications for oceanography and paleoceanography. Chem. Geol. 198, 305–334.

Buening, N., Carlson, S.J., 1992. Geochemical investigation of growth in selected Recent articulate brachiopods. Lethaia 25, 331–345.

Buening, N., Carlson, S.J., Spero, H.J., Lee, D.E., 1998. Evidence for the Early Oligocene formation of a proto-Subtropical Convergence from oxygen isotope records of New Zealand Paleogene brachiopods. Palaeogeogr. Palaeoclimatol. Palaeoecol. 138, 43–68.

Carpenter, S.J., Lohmann, K.C., 1995. $\delta^{18}O$ and $\delta^{13}C$ values of modern brachiopod shells. Geochim. Cosmochim. Acta 59, 3749–3764.

De La Rocha, C.L., DePaolo, D.J., 2000. Isotopic evidence for variations in the marine calcium cycle over the Cenozoic. Science 289, 1176–1178.

Eisenhauer, A., Nägler, T.F., Stille, P., Kramers, J., Gussone, N., Bock, B., Fietzke, J., Hippler, D., Schmitt, A.-D., 2004. Proposal for an international agreement on Ca notation as result of the discussions from the workshops on stable isotope measurements in Davos (Goldschmidt 2002) and Nice (EGS-AGU-EUG 2003). Geostandards Geoanal. Res. 28, 149–151.

Emig, C., 1987. Offshore brachiopods investigated by submersible. J. Exp. Mar. Biol. Ecol. 108, 261–273.

Emig, C.C., 1989a. Distribution bathymétrique et spatiale des populations de *Gryphus vitreus* (brachiopode) sur la marge continentale (Nord-Ouest Méditerranée). Oceanol. Acta 12, 205–209.

Emig, C.C., 1989b. Distributional patterns along the Mediterranean continental margin (upper bathyal) using *Gryphus vitreus* (Brachiopoda) densities. Palaeogeogr. Palaeoclimatol. Palaeoecol. 71, 253–256.

Emig, C.C., 1990. Examples of post-mortality alteration in Recent brachiopod shells and (paleo)ecological consequences. Mar. Biol. 104, 233–238.

Epstein, S., Buchsbaum, R., Lowenstam, H.A., Urey, H.C., 1953. Revised carbonate-water isotopic temperature scale. Geol. Soc. Amer. Bull. 64, 1315–1326.

Fantle, M.S., DePaolo, D.J., 2005. Variations in the marine Ca cycle over the past 20 million years. Earth Planet. Sci. Lett. 237, 102–117.

Farkaš, J., Böhm, F., Wallmann, K., Blenkinsop, J., Eisenhauer, A., van Geldern, R., Munnecke, A., Voigt, S., Veizer, J., 2007a. Calcium isotope record of Phanerozoic oceans: implications for chemical evolution of seawater and its causative mechanisms. Geochim. Cosmochim. Acta 71, 5117–5134.

Farkaš, J., Buhl, D., Blenkinsop, J., Veizer, J., 2007b. Evolution of the oceanic calcium cycle during the late Mesozoic: evidence from $\delta^{44/40}Ca$ of marine skeletal carbonates. Earth Planet. Sci. Lett. 253, 96–111.

Gaspard, D., 1986. Aspects figurés de la biominéralisation unités de base de la sécrétion carbonatée chez les Terebratulida actuels. Biostratigr. Paléozoïque Brest 4, 77–83.

Griffith, E.M., Paytan, A., Caldeira, K., Bullen, T.D., Thomas, E., 2008. A dynamic marine calcium cycle during the past 28 million years. Science 322, 1671–1674.

Grossman, E.L., Mii, H.S., Zhang, C., Yancey, T.E., 1996. Chemical variation in Pennsylvanian brachiopod shells — diagenetic, taxonomic microstructural, and seasonal effects. J. Sediment. Res. 66, 1011–1022.

Gussone, N., Böhm, F., Eisenhauer, A., Dietzel, M., Heuser, A., Teichert, B.M.A., Reitner, J., Worheide, G., Dullo, W.-C., 2005. Calcium isotope fractionation in calcite and aragonite. Geochim. Cosmochim. Acta 69, 4485–4494.

Gussone, N., Eisenhauer, A., Heuser, A., Dietzel, M., Bock, B., Böhm, F., Spero, H.J., Lea, D.W., Bijma, J., Nägler, T.F., 2003. Model for kinetic effects on calcium isotope fractionation ($\delta^{44}Ca$) in inorganic aragonite and cultured planktonic foraminifera. Geochim. Cosmochim. Acta 67, 1375–1382.

Gussone, N., Eisenhauer, A., Tiedemann, R., Haug, G.H., Heuser, A., Bock, B., Nägler, T.F., Müller, A., 2004. Reconstruction of Caribbean Sea surface temperature and salinity fluctuations in response to the Pliocene closure of the Central American Gateway and radiative forcing, using $\delta^{44/40}Ca$, $\delta^{18}O$ and Mg/Ca ratios. Earth Planet. Sci. Lett. 227, 201–214.

Gussone, N., Hönisch, B., Heuser, A., Eisenhauer, A., Spindler, M., Hemleben, C., 2009. A critical evaluation of calcium isotope ratios in tests of planktonic foraminifers. Geochim. Cosmochim. Acta. 73, 7241–7255.

Gussone, N., Langer, G., Geisen, M., Steel, B.A., Riebesell, U., 2007. Calcium isotope fractionation in coccoliths of cultured *Calcidiscus leptoporus*, *Helicosphaera carteri; Syracospaera pulchra and Umbilicosphaera foliosa*. Earth Planet. Sci. Lett. 260, 5505–5515.

Gussone, N., Langer, G., Thoms, S., Nehrke, G., Eisenhauer, A., Riebesell, U., Wefer, G., 2006. Cellular calcium pathways and isotope fractionation in *Emiliania huxleyi*. Geology 34, 625–628.

Heuser, A., Eisenhauer, A., Böhm, F., Wallmann, K., Gussone, N., Pearson, P.N., Nägler, T.F., Dullo, W.C., 2005. Calcium Isotope ($\delta^{44/40}Ca$) Variations of Neogene planktonic foraminifera. Paleoceanography 20, PA2013.

Heuser, A., Eisenhauer, A., Gussone, N., Bock, B., Hansen, B.T., Nägler, T.F., 2002. Measurement of calcium isotopes ($\delta^{44}Ca$) using a multicollector TIMS technique. Int. J. Mass Spectrom. 220, 385–397.

Hippler, D., Eisenhauer, A., Nägler, T.F., 2006. Tropical Atlantic SST history inferred from Ca isotope thermometry over the last 140 ka. Geochim. Cosmochim. Acta 70, 90–100.

Hippler, D., Kozdon, R., Darling, K.F., Eisenhauer, A., Nägler, T.F., 2009. Calcium isotopic composition of high-latitude proxy carrier *Neogloboquadrina pachyderma* (sin.). Biogeosciences 6, 1–14.

Hippler, D., Schmitt, A.-D., Gussone, N., Heuser, A., Stille, P., Eisenhauer, A., Nägler, T.F., 2003. Ca isotopic composition of various standards and seawater. Geostand. Newsl. 27, 13–19.

Hippler, D., Villa, I.M., Nägler, T.F., Kramers, J.D., 2004. A ghost haunts mass spectrometry: real isotope fractionation or analytical paradox? Geochim. Cosmochim. Acta 68, A215.

Immenhauser, A., Holmden, C., Patterson, W.P., 2008. Interpreting the carbon-isotope record of ancient shallow Epeiric Seas: lessons from the Recent. In: Pratt, B.R., Holden, C. (Eds.), Dynamics of Epeiric Seas, vol. 48. Geological Association of Canada, Special Publication, pp. 137–174.

Immenhauser, A., Kenter, J.A.M., Ganssen, G., Bahamonde, J.R., Van Vliet, A., Saher, M.H., 2002. Origin and significance of isotope shifts in Pennsylvanian carbonates (Asturias, NW Spain). J. Sediment. Res. 72, 82–94.

Immenhauser, A., Nägler, T.F., Steuber, T., Hippler, D., 2005. A critical assessment of mollusk $^{18}O/^{16}O$, Mg/Ca, and $^{44}Ca/^{40}Ca$ ratios as proxies for Cretaceous seawater temperature seasonality. Palaeogeogr. Palaeoclimatol. Palaeoecol. 215, 221–237.

Jackson, S., 2008. LAMTRACE data reduction software for LA-ICP-MS. In: Sylvester, P. (Ed.), Laser ablation ICP-MS in the Earth Sciences: Current practices and outstanding issues. Short Course Series - Mineral. Assoc. Can., vol. 40. Mineral. Assoc. Can, pp. 305–307.

Klein, R.T., Lohmann, K.C., Thayer, C.W., 1996a. Bivalve skeletons record sea-surface temperature and $\delta^{18}O$ via Mg/Ca and $^{18}O/^{16}O$ ratios. Geology 24, 415–418.

Klein, R.T., Lohmann, K.C., Thayer, C.W., 1996b. Sr/Ca and $^{13}C/^{12}C$ ratios in skeletal calcite of *Mytilus trossulus*: covariation with metabolic rate, salinity, and carbon isotopic composition of seawater. Geochim. Cosmochim. Acta 60, 4207–4221.

Logan, A., Noble, J.P.A., 1971. A Recent shallow-water brachiopod community from the Bay of Fundy. Marit. Sediments 7, 85–91.

MacKinnon, D.I., Williams, A., 1974. Shell structure of terebratulid brachiopods. Palaeontology 17, 179–202.

Marriott, C.S., Henderson, G.M., Belshaw, N.S., Tudhope, A.W., 2004. Temperature dependence of $\delta^{7}Li$, $\delta^{44}Ca$ and Li/Ca during growth of calcium carbonate. Earth and Planet. Sci. Lett. 222, 615–624.

McConnaughey, T., 1989a. ^{13}C and ^{18}O isotopic disequilibrium in biological carbonates: I Patterns. Geochim. Cosmochim. Acta 53, 151–162.

McConnaughey, T., 1989b. ^{13}C and ^{18}O isotopic disequilibrium in biological carbonates: II In vitro simulation of kinetic isotope effects. Geochim. Cosmochim. Acta 53, 163–171.

McConnaughey, T.A., Burdett, J., Whelan, J.F., Paull, C.K., 1997. Carbon isotopes in biological carbonates: respiration and photosynthesis. Geochim. Cosmochim. Acta 61, 611–622.

Mii, H.S., Grossman, E.L., 1994. Late Pennsylvanian seasonality reflected in the ^{18}O and elemental composition of a brachiopod shell. Geology 22, 661–664.

Nägler, T.F., Eisenhauer, A., Müller, A., Hemleben, C., Kramers, J., 2000. The δ^{44}Ca-temperature calibration on fossil and cultured *Gobigerinoides sacculifer*: New tool for reconstruction of past sea surface temperatures. Geochem. Geophys. Geosyst. 1. doi:10.1029/2000GC000091.
Noble, J.P.A., Logan, A., Webb, G.R., 1976. The Recent *Terebratulina* community in the rocky subtidal zone of the Bay of Fundy, Canada. Lethaia 9, 1–17.
Parkinson, D., Curry, G.B., Cusack, M., Fallick, A.E., 2005. Shell structure, patterns and trends of oxygen and carbon stable isotopes in modern brachiopod shells. Chem. Geol. 219, 193–235.
Pettke, T., 2008. Analytical protocols for element concentration and isotope ratio measurements in fluid inclusions by LA-(MC)-ICP-MS. In: Sylvester, P. (Ed.), Laser ablation ICP-MS in the Earth Sciences: Current practices and outstanding issues: Short Course Series - Mineral. Assoc. Can., vol. 40, pp. 189–218.
Popp, B.N., Anderson, T.F., Sandberg, P.A., 1986. Brachiopods as indicators of original isotopic compositions in some Paleozoic limestones. GSA Bull. 97, 1262–1269.
Romanek, C.S., Grossman, E.L., 1989. Stable isotope profiles of *Tridacna maxima* as environmental indicators. Palaios 4, 402–413.
Schmitt, A.-D., Bracke, G., Stille, P., Kiefel, B., 2001. The calcium isotope composition of modern seawater determined by thermal ionisation mass spectrometry. Geostand. Newsl. 25, 267–275.
Schmitt, A.-D., Stille, P., Vennemann, T., 2003. Variations of the ^{44}Ca/^{40}Ca ratio in seawater during the past 24 million years: evidence from δ^{44}Ca and δ^{18}O values of Miocene phosphates. Geochim. Cosmochim. Acta 67, 2607–2614.
Shenton, F.H., Horton, D.B., 1973. Literature review for the Marine Environmental data for Eastport, Maine. The Research Institute for the Gulf of Maine, Vol. 1: vi + 130 pp, Vol. 2: Appendices I-XV.
Silva-Tamayo, J.C., Nägler, T.F., Villa, I.M., Kyser, K., Sial, A.N., Narbonne, G., James, N.P., Da Silva Filho, M.A., 2007. Global Ca-isotope signatures in post-Snowball Earth cap-carbonates. Goldschmidt Conference, Cologne, Germany: Geochim. Cosmochim. Acta, vol. 71, p. A938-A938. Suppl. S.
Sime, N.G., De La Rocha, C.L., Galy, A., 2005. Negligible temperature dependence of calcium isotope fractionation in 12 species of planktonic foraminifera. Earth Planet. Sci. Lett. 232, 51–66.
Sime, N.G., De La Rocha, C.L., Tipper, E.T., Tripati, A., Galy, A., Bickle, M.J., 2007. Interpreting the Ca isotope record of marine biogenic carbonates. Geochim. Cosmochim. Acta 71, 3979–3989.
Skulan, J., DePaolo, D.J., Owens, T.L., 1997. Biological control of calcium isotopic abundances in the global calcium cycle. Geochim. Cosmochim. Acta 61, 2505–2510.
Soper, D., 2009. The Free Statistics Calculators Website, Online Software. http://www.danielsoper.com/statcalc/.
Spero, H.J., Lea, D.W., 1996. Experimental determination of stable isotope variability in *Globigerina bulloides*: implications for paleoceanographic reconstructions. Mar. Micropaleontol. 28, 231–246.
Steuber, T., Buhl, D., 2006. Calcium-isotope fractionation in selected modern and ancient marine carbonates. Geochim. Cosmochim. Acta 70, 5507–5521.
Steuber, T., Veizer, J., 2002. Phanerozoic record of plate tectonic control of seawater chemistry and carbonate sedimentation. Geol. Soc. Amer. 30, 1123–1126.
Tang, J., Dietzel, M., Böhm, F., Köhler, S.J., Eisenhauer, A., 2008. Sr^{2+}/Ca^{2+} and ^{44}Ca/^{40}Ca fractionation during inorganic calcite formation: II Ca isotopes. Geochim. Cosmochim. Acta 72, 3733–3745.
Weiner, S., Dove, P.M., 2003. An overview of biomineralization processes and the problem of the vital effect. Rev. Mineral. Geochem. 54, 1–31.
Williams, A., 1968. Evolution of the shell structure of articulate brachiopods. Spec. Pap. Palaeontol. 2, 1–55.
Williams, A., 1973. The secretion and structural evolution of the shell of thecideidine brachiopods. Philos. Trans. R. Soc. Lond., B Biol. Sci. 264, 439–478.
Wilson-Finelli, A., Chandler, G.T., Spero, H.J., 1998. Stable isotope behavior in paleoceanographically important benthic foraminifera: Results from microcosm culture experiments. J. Foraminiferal Res. 28, 312–320.
Wolf, K.H., Chilingar, G.V., Beales, F.W., 1967. Elemental composition of carbonate skeletons, minerals and sediments. In: Chilingar, G.V., et al. (Ed.), Carbonate rocks, physcial and chemical aspects: Developments in Sedimentology, vol. 9B. Elsevier, Amsterdam, pp. 23–151.
Zhu, P., Macdougall, J.D., 1998. Calcium isotopes in the marine environment and the oceanic calcium cycle. Geochim. Cosmochim. Acta 62, 1691–1698.